Taylor & Francis
Taylor & Francis Group

Research in Sports Medicine
An International Journal

ISSN: (Print) (Online) Journal homepage: https://www.tandfonline.com/loi/gspm20

Hamstring musculotendon mechanics of prospectively injured elite rugby athletes

Claire Kenneally-Dabrowski, Nicholas A.T. Brown, Benjamin G. Serpell, Diana Perriman, Wayne Spratford, Ashlee Sutherland, Mark Pickering & Adrian K.M. Lai

To cite this article: Claire Kenneally-Dabrowski, Nicholas A.T. Brown, Benjamin G. Serpell, Diana Perriman, Wayne Spratford, Ashlee Sutherland, Mark Pickering & Adrian K.M. Lai (16 Mar 2023): Hamstring musculotendon mechanics of prospectively injured elite rugby athletes, Research in Sports Medicine, DOI: 10.1080/15438627.2023.2189115

To link to this article: https://doi.org/10.1080/15438627.2023.2189115

Published online: 16 Mar 2023.

RESEARCH IN SPORTS MEDICINE
https://doi.org/10.1080/15438627.2023.2189115

Routledge
Taylor & Francis Group

Hamstring musculotendon mechanics of prospectively injured elite rugby athletes

Claire Kenneally-Dabrowski[a,b,c], Nicholas A.T. Brown[d], Benjamin G. Serpell[e,f,g], Diana Perriman[a,h], Wayne Spratford[d,i], Ashlee Sutherland[e,j], Mark Pickering[h,k] and Adrian K.M. Lai[l]

[a]ANU Medical School, Australian National University, Canberra, ACT, Australia; [b]Movement Science, Australian Institute of Sport, Canberra, ACT, Australia; [c]Centre for Sports Research, School of Exercise and Nutrition Sciences, Deakin University, Burwood, Australia; [d]Faculty of Health, University of Canberra Research Institute for Sport and Exercise, Canberra, ACT, Australia; [e]Football Department, Brumbies Rugby, Canberra, ACT, Australia; [f]Football Department, Geelong Football Club, Geelong, VIC, Australia; [g]School of Science and Technology, University of New England, Armidale, NSW, Australia; [h]Trauma and Orthopaedic Research Unit, Canberra Hospital, Canberra, ACT, Australia; [i]Discipline of Sport and Exercise Science, Faculty of Health, University of Canberra, Canberra, ACT, Australia; [j]Discipline of Physiotherapy, Faculty of Health, University of Canberra, Bruce, ACT, Australia; [k]School of Engineering and Information Technology, University of New South Wales at the Australian Defence Force Academy, Canberra, Australia; [l]Product Innovation, lululemon Athletica, Vancouver, BC, Canada

ABSTRACT

The musculotendon mechanics of the hamstrings during high-speed running are thought to relate to injury but have rarely been examined in the context of prospectively occurring injury. This prospective study describes the hamstring musculotendon mechanics of two elite rugby players who sustained hamstring injuries during on-field running. Athletes undertook biomechanical analyses of high-speed running during a Super Rugby pre-season, prior to sustaining hamstring injuries during the subsequent competition season. The biceps femoris long head muscle experienced the greatest strain of all hamstring muscles during the late swing phase. When expressed relative to force capacity, biceps femoris long head also experienced the greatest musculotendon forces of all hamstring muscles. Musculotendon strain and force may both be key mechanisms for hamstring injury during the late swing phase of running.

ARTICLE HISTORY
Received 25 August 2022
Accepted 20 February 2023

KEYWORDS
Muscle injuries; musculoskeletal modelling; case report; biceps femoris long head; biomechanics; hamstrings; injury

Introduction

Hamstring injuries remain the most prevalent and costly injury in many running-based field sports (Brooks et al., 2005; Ekstrand et al., 2016), with the majority occurring during high-speed running and affecting the biceps femoris long head (BFlh) muscle (Askling et al., 2013; Kenneally Dabrowski, Serpell, et al., 2019). These running-based hamstring injuries typically occur during the late swing phase when the BFlh undergoes a large eccentric contraction to decelerate the rotation of the shank (C. J. B. Kenneally Dabrowski et al., 2019). While some

CONTACT Claire Kenneally-Dabrowski claire.kenneallydabrowski@deakin.edu.au Centre for Sport Research, School of Exercise and Nutrition Sciences, Deakin University, 75 Pigdons Road, Waurn Ponds, VIC, 3216, Australia

insights into the mechanism of injury at the musculotendon level have been gained from serendipitous measurement during an injury (Heiderscheit et al., 2005; Schache et al., 2009, 2010), data from athletes prior to on-field high-speed running injuries have not been reported. Further, muscle-tendon unit (MTU) forces of the individual hamstring muscles prior to injury have also not yet been reported; only net hamstring forces (Heiderscheit et al., 2005; Schache et al., 2009, 2010). Data describing the hamstring musculotendon mechanics of injured athletes prior to injury are pivotal to better understanding the mechanism of injury.

The aim of this study was to describe the hamstring musculotendon mechanics of two athletes who prospectively sustained hamstring injuries while running.

Materials and methods

Two elite male rugby union players (Athlete A, height, 192.5 cm; weight, 97.9 kg; age, 31 yrs; position, centre; Athlete B, height, 202.1 cm; weight, 115.2 kg; age, 25 yrs; position, lock) completed biomechanical running analyses during pre-season as part of a larger study (Kenneally Dabrowski, Brown, et al. 2019). Both athletes sustained hamstring injuries in the following competition season. Written informed consent was provided by both athletes, and the study was approved by the human research ethics committees of the Australian National University and the Australian Institute of Sport (approval no: 2016/674).

Pre-season data collection

Biomechanical running analyses took place on an indoor synthetic track at the Australian Institute of Sport. Reflective markers were placed on specific anatomical landmarks (see Kenneally Dabrowski, Brown, et al. (2019)) before players completed three maximal 50-m sprints. Trajectory data were collected via a 20-camera three-dimensional motion analysis system (VICON, Oxford Metrics LTD., Oxford, United Kingdom) sampling at 250 Hz, positioned around the 30–50-m region of the sprint. Ground reaction forces were collected via eight 900 × 600 mm force plates (Kistler Instrument Corp., Winterthur, Switzerland) sampling at 1000 Hz.

MRI scans were performed on each athletes' hamstrings in the 48 hours prior to the running analysis. Athletes were positioned supine within a Skyra 3-Tesla MRI scanner (Siemens, Erlangen, Germany) and a T1 Vibe DIXON sequence was acquired (slice thickness, 1.6 mm; distance factor, 20%; FOV 500 × 500; FOV phase, 100%; base resolution, 320; matrix, 320 × 320; TE, 2.46; TR 5.73). The proximal and distal boundaries of the scan were aligned to the ischial tuberosity and lateral head of the fibula, respectively.

In-season hamstring injury cases

Athlete A sustained an injury at the distal myofascial junction of the right BFlh during competition, 139 days after the running analysis. This injury was assessed via MRI as a grade 2a hamstring strain (Pollock et al., 2014) and resulted in 20 days lost from full training and competition. Athlete A had a history of three left hamstring injuries which occurred 29–44 months prior to the running analysis, and no prior right hamstring injuries in the five years preceding this study. Athlete B sustained a right hamstring injury during

competition 192 days after the running analysis. This injury was not assessed with MRI, however it resulted in 28 days lost from full training and competition. Athlete B had no history of hamstring injuries in the five years preceding the running analysis.

Data analysis

Pre-season MRI data were manually segmented using a custom Matlab application, which has been previously used to segment and create 3D reconstructions of cervical spine muscles (Au et al., 2016). Muscle borders were traced on axial slices for all four hamstring muscles and these cross-sectional areas were used to calculate whole muscle volume. Physiological cross-sectional area (PCSA) was then calculated, defined as muscle volume (cm^3)/optimal fibre length (cm) (Friederich & Brand, 1990).

A musculoskeletal model was scaled to each athletes' anthropometry and used to predict hamstring MTU mechanics during the late swing phase of sprinting (Lai et al., 2017). All simulations were performed in OpenSim v3.3 (see Appendix A for extended modelling methods). Hamstring MTU force was normalized to body mass (N/kg) and to PCSA of each muscle, enabling examination of MTU force relative to the muscle's capacity for load. MTU lengths were expressed as strain (percentage change in length from a standing pose), where positive strain values reflect an increase in length. MTU velocity was calculated as the derivative of length with respect to time. MTU power was the product of MTU force and velocity, expressed relative to body mass (W/kg). The running velocity of each athlete was calculated from the centre of the pelvis segment across a single, full stride. All data were normalized to 100% of the late swing phase of the right leg and averaged across trials.

Results

Running velocities for Athletes A and B were 9.05 m/s and 8.53 m/s respectively. Peak MTU strain was greatest in the BFlh muscle, while ST displayed the greatest lengthening velocity, for both athletes. Peak MTU force (N/kg) was greatest for the SM for both athletes. However, when normalized to PCSA, MTU force (N/PCSA) was greatest in the BFlh for Athlete A, and similar for SM and BFlh for Athlete B. Peak power absorption was largest in BFlh for Athlete A, and SM for Athlete B (Figure 1 and Table 1). Additional modelling outcomes are presented in Appendix B.

Discussion

This study sought to describe hamstring MTU mechanics of two athletes who prospectively sustained running-based hamstring injuries. Peak MTU strain during the late swing phase of running was greatest in the BFlh muscle for both athletes. This is consistent with previously reported data (Chumanov et al., 2011; Heiderscheit et al., 2005; Schache et al., 2009, 2012; Thelen, Chumanov, Hoerth, et al., 2005). Schache et al. (2012) proposed that strain is the primary mechanism for injury, as BFlh strain is greater than in the other hamstring muscles. On these grounds, our data supports this theory and may assist in explaining why BFlh is the most commonly injured hamstring muscle while running (Schache et al., 2012).

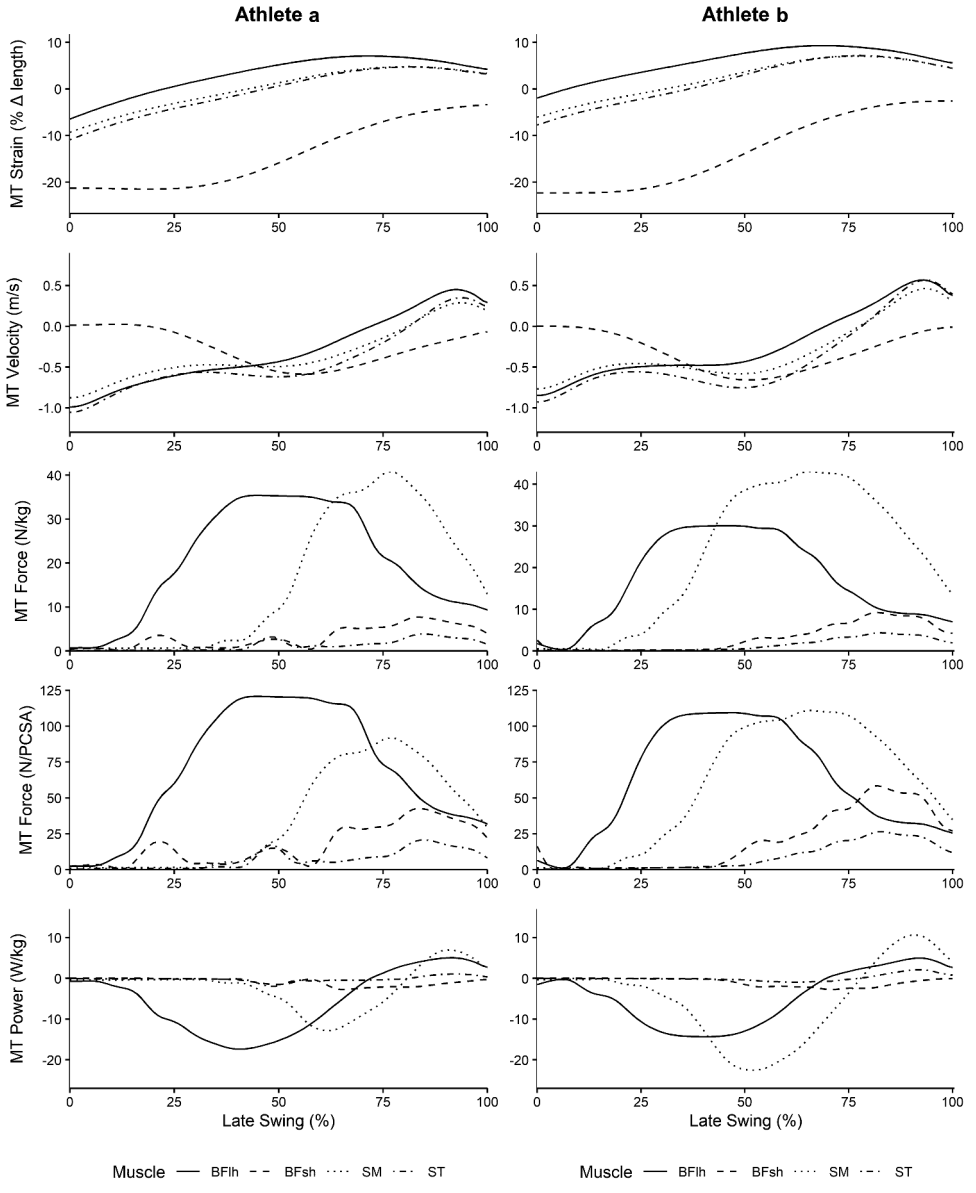

Figure 1. Musculotendon (MT) strain (%), velocity (m/s), force (N/kg and (N/cm3) and power (W/kg) for each of the four hamstring muscles, across the late swing phase, for athletes a and B. Late swing phase was defined as beginning at peak knee flexion (0%) and ending at foot contact (100%).

Muscle-tendon unit lengthening velocities were greatest in ST and occurred during initial knee extension at the beginning of late swing phase (Schache et al., 2012). This observation was unsurprising as the long fascicles of ST mean it's architecture is well designed for large, rapid excursions in length (Kellis et al., 2012; Lieber & Friden, 2000) and therefore may be more resistant to strain injury.

The greatest MTU force (N/kg) was found for the SM muscle, which is consistent with data in healthy populations (Chumanov et al., 2011; Schache et al., 2012). The SM

Table 1. Peak MTU strain, velocity, force and power absorption during the late swing phase for each hamstring muscle.

	BFlh	BFsh	SM	ST
Athlete A				
Peak strain (% change from static pose)#	7.07	−3.39	4.77	4.73
Resting length (m)*	0.47	0.25	0.46	0.51
Peak lengthening velocity (m/s)	−0.99	−0.59	−0.88	−1.05
Peak force/BW (N/kg)	35.40	7.70	40.80	3.86
Peak force/PCSA (N/PCSA)	120.80	42.71	91.91	20.73
Peak power absorption (W/kg)	−17.38	−2.78	−12.82	−1.98
Athlete B				
Peak strain (% change from static pose)#	9.31	−2.60	7.04	7.15
Resting length (m)*	0.49	0.26	0.48	0.53
Peak lengthening velocity (m/s)	−0.85	−0.66	−0.77	−0.93
Peak force/BW (N/kg)	30.06	9.22	43.03	4.35
Peak force/PCSA (N/PCSA)	109.38	58.53	110.89	26.51
Peak power absorption (W/kg)	−14.34	−2.76	−22.55	−0.96

BFlh, biceps femoris long head; BFsh, biceps femoris short head; SM, semimembranosus; ST, semitendinosus. Note: Late swing phase was defined as beginning at peak knee flexion and ending at foot contact.

#Positive strain values reflect an increase in length from the resting length, and negative values represent a decrease in length from the resting length.

*MTU length during the static pose.

muscle has the largest PCSA of the hamstring muscles, and is therefore well designed to produce large forces (Kellis et al., 2012). However, when MTU force was normalized to PCSA, BFlh load was equal to, or greater than, SM load. PCSA is directly proportional to maximum isometric force and is therefore an appropriate measure of a muscle's force generating capacity (Lieber & Friden, 2000). By normalizing MTU force to PCSA, we can better understand how the hamstring MTU force during late swing relates to each muscle's capacity to produce force. Thus, our results suggest that the load experienced by the BFlh during late swing could be a key factor in its propensity for injury while running.

The two athletes differed in terms of which muscle demonstrated the greatest power absorption, with Athlete A demonstrating highest power absorption in BFlh, whereas for Athlete B it was SM. Athlete B's MTU power profile was a result of high SM force and high SM velocity during late swing and is consistent previous data in healthy sprinters (Schache et al., 2012). Slight variations in MTU force, and the timing for peak MTU force relative to the second peak in MTU velocity observed from Athlete A contributed to the discrepancy observed between the two participants, which was amplified when calculating MTU power.

The findings of this study provide insight into potential hamstring injury mechanisms at the musculotendon level. Future research should also consider how BFlh musculotendon force relative to capacity and BFlh strain relate to more readily measurable parameters. In a recent concept mapping study, a panel of experts noted that the ability of an athlete to adapt to musculotendon stress and strain during high-speed running was important for hamstring injury risk reduction (Kalema et al., 2021). However, experts had relatively low confidence that these characteristics could be addressed in a hamstring injury prevention program. This highlights the need to understand how other hamstring injury risk factors which can be more easily "coached" in an applied setting relate to musculotendon mechanics. In particular, it would be valuable to understand how BFlh musculotendon mechanics relate to joint level kinematics.

These data are not without methodological limitations. The model is sensitive to the musculotendon input parameters. While each model was scaled to individual athlete anthropometry, subject-specific inputs such as fibre length, tendon slack length and maximum isometric force were not available. Further, the stability of running mechanics and hamstring musculotendon properties of athletes over time are unknown. Therefore, we cannot be certain that athlete kinematics and musculotendon parameters did not change between the running analyses and injury occurrences. It should also be acknowledged that hamstring injuries are multifactorial, and other factors such as training load, age and previous injury may influence injury risk. Notably, Athlete A had a history of three prior left hamstring injuries. Previous research has described changes in muscle architecture (Timmins et al., 2015) and running mechanics (Daly et al., 2016) following hamstring injury and it is possible that this athlete's history of left hamstring injuries may influence their running mechanics bilaterally.

This is the first study to report MTU forces of individual hamstring muscles prior to injury. Prior to this study only net hamstring MTU forces had been reported (Schache et al., 2010). Thus, our rare data provides considerable insight into the potential mechanisms for injury at the musculotendon level. Specifically, the normalization of hamstring MTU forces to muscle PCSA is novel to this study and it reveals the potential importance of BFlh muscle load relative to capacity as a mechanism for hamstring injury during late swing. BFlh strain was also identified as a potential mechanism for hamstring injury. It is likely that both the MTU strain and MTU load relative to capacity contribute to the propensity for injury to the BFlh.

Disclosure statement

No potential conflict of interest was reported by the authors.

Funding

This research was supported by an Australian Government Research Training Scholarship. This research did not receive any other funding or any grant support.

ORCID

Claire Kenneally-Dabrowski http://orcid.org/0000-0001-5433-5082
Benjamin G. Serpell http://orcid.org/0000-0002-9067-2948
Wayne Spratford http://orcid.org/0000-0002-6207-8829

Data availability statement

The data that supports the findings of this study are available in the appendices of this article.

References

Askling, C. M., Tengvar, M., & Thorstensson, A. (2013). Acute hamstring injuries in Swedish elite football: A prospective randomised controlled clinical trial comparing two rehabilitation protocols. *British Journal of Sports Medicine*, *47*(15), 953–959. https://doi.org/10.1136/bjsports-2013-092165

Au, J., Perriman, D. M., Pickering, M. R., Buirski, G., Smith, P. N., & Webb, A. L. (2016). Magnetic resonance imaging atlas of the cervical spine musculature. *Clinical Anatomy*, *29*(5), 643–659. https://doi.org/10.1002/ca.22731

Brooks, J. H., Fuller, C. W., Kemp, S. P., & Reddin, D. B. (2005). Epidemiology of injuries in English professional rugby union: Part 1 match injuries. *British Journal of Sports Medicine*, *39*(10), 757–766. https://doi.org/10.1136/bjsm.2005.018135

Chumanov, E. S., Heiderscheit, B. C., & Thelen, D. G. (2011). Hamstring musculotendon dynamics during stance and swing phases of high-speed running. *Medicine & Science in Sports & Exercise*, *43* (3), 525–532. https://doi.org/10.1249/MSS.0b013e3181f23fe8

Daly, C., McCarthy Persson, U., Twycross Lewis, R., Woledge, R. C., & Morrissey, D. (2016). The biomechanics of running in athletes with previous hamstring injury: A case-control study. *Scandinavian Journal of Medicine & Science in Sports*, *26*(4), 413–420. https://doi.org/10.1111/sms.12464

Ekstrand, J., Waldén, M., & Hägglund, M. (2016). Hamstring injuries have increased by 4% annually in men's professional football, since 2001: A 13-year longitudinal analysis of the UEFA Elite Club injury study. *British Journal of Sports Medicine*, *50*(12), 731–737. https://doi.org/10.1136/bjsports-2015-095359

Friederich, J. A., & Brand, R. A. (1990). Muscle fiber architecture in the human lower limb. *Journal of Biomechanics*, *23*(1), 91–95. https://doi.org/10.1016/0021-9290(90)90373-B

Handsfield, G. G., Meyer, C. H., Hart, J. M., Abel, M. F., & Blemker, S. S. (2014). Relationships of 35 lower limb muscles to height and body mass quantified using MRI. *Journal of Biomechanics*, *47*(3), 631–638. https://doi.org/10.1016/j.jbiomech.2013.12.002

Heiderscheit, B. C., Hoerth, D. M., Chumanov, E. S., Swanson, S. C., Thelen, B. J., & Thelen, D. G. (2005). Identifying the time of occurrence of a hamstring strain injury during treadmill running: A case study. *Clinical Biomechanics*, *20*(10), 1072–1078. https://doi.org/10.1016/j.clinbiomech.2005.07.005

Higashihara, A., Nagano, Y., Ono, T., & Fukubayashi, T. (2015). Differences in activation properties of the hamstring muscles during overground sprinting. *Gait & Posture*, *42*(3), 360–364. https://doi.org/10.1016/j.gaitpost.2015.07.002

Kalema, R. N., Duhig, S. J., Williams, M. D., Donaldson, A., & Shield, A. J. (2021). Sprinting technique and hamstring strain injuries: A concept mapping study. *Journal of Science and Medicine in Sport*, *25*(3), 209–215. https://doi.org/10.1016/j.jsams.2021.09.007

Kellis, E., Galanis, N., Kapetanos, G., & Natsis, K. (2012). Architectural differences between the hamstring muscles. *Journal of Electromyography and Kinesiology*, *22*(4), 520–526. https://doi.org/10.1016/j.jelekin.2012.03.012

Kenneally Dabrowski, C. J. B., Brown, N. A. T., Lai, A. K. M., Perriman, D., Spratford, W., & Serpell, B. G. (2019). Late swing or early stance? A narrative review of hamstring injury mechanisms during high-speed running. *Scandinavian Journal of Medicine & Science in Sports*, *29*(8), 1083–1091. https://doi.org/10.1111/sms.13437

Kenneally Dabrowski, C., Brown, N. A., Warmenhoven, J., Serpell, B. G., Perriman, D., Lai, A. K., & Spratford, W. (2019). Late swing running mechanics influence hamstring injury susceptibility in elite rugby athletes: A prospective exploratory analysis. *Journal of Biomechanics*, *92*, 112–119. https://doi.org/10.1016/j.jbiomech.2019.05.037

Kenneally Dabrowski, C., Serpell, B. G., Spratford, W., Lai, A. K., Field, B., Brown, N. A., Thomson, M., & Perriman, D. (2019). A retrospective analysis of hamstring injuries in elite rugby athletes: More severe injuries are likely to occur at the distal myofascial junction. *Physical Therapy in Sport*, *38*, 192–198. https://doi.org/10.1016/j.ptsp.2019.05.009

Kyröläinen, H., Komi, P. V., & Belli, A. (1999). Changes in muscle activity patterns and kinetics with increasing running speed. *The Journal of Strength & Conditioning Research*, *13*(4), 400–406. https://doi.org/10.1519/00124278-199911000-00017

Lai, A. K., Arnold, A. S., & Wakeling, J. M. (2017). Why are antagonist muscles co-activated in my simulation? A musculoskeletal model for analysing human locomotor tasks. *Annals of Biomedical Engineering*, *45*(12), 2762–2774. https://doi.org/10.1007/s10439-017-1920-7

Lieber, R. L., & Friden, J. (2000). Functional and clinical significance of skeletal muscle architecture. *Muscle & Nerve*, *23*(11), 1647–1666. doi:10.1002/1097-4598(200011)23:11<1647:AID-MUS1>3.0.CO;2-M

Pollock, N., James, S. L., Lee, J. C., & Chakraverty, R. (2014). British athletics muscle injury classification: A new grading system. *British Journal of Sports Medicine*, *48*(18), 1347–1351. https://doi.org/10.1136/bjsports-2013-093302

Rajagopal, A., Dembia, C. L., DeMers, M. S., Delp, D. D., Hicks, J. L., & Delp, S. L. (2016). Full-body musculoskeletal model for muscle-driven simulation of human gait. *IEEE Transactions on Biomedical Engineering*, *63*(10), 2068–2079. https://doi.org/10.1109/TBME.2016.2586891

Schache, A. G., Dorn, T. W., Blanch, P. D., Brown, N. A., & Pandy, M. G. (2012). Mechanics of the human hamstring muscles during sprinting. *Medicine & Science in Sports & Exercise*, *44*(4), 647–658. https://doi.org/10.1249/MSS.0b013e318236a3d2

Schache, A. G., Kim, H. J., Morgan, D. L., & Pandy, M. G. (2010). Hamstring muscle forces prior to and immediately following an acute sprinting-related muscle strain injury. *Gait & Posture*, *32*(1), 136–140. https://doi.org/10.1016/j.gaitpost.2010.03.006

Schache, A. G., Wrigley, T. V., Baker, R., & Pandy, M. G. (2009). Biomechanical response to hamstring muscle strain injury. *Gait & Posture*, *29*(2), 332–338. https://doi.org/10.1016/j.gaitpost.2008.10.054

Thelen, D. G., & Anderson, F. C. (2006). Using computed muscle control to generate forward dynamic simulations of human walking from experimental data. *Journal of Biomechanics*, *39*(6), 1107–1115. https://doi.org/10.1016/j.jbiomech.2005.02.010

Thelen, D. G., Chumanov, E. S., Best, T. M., Swanson, S. C., & Heiderscheit, B. C. (2005). Simulation of biceps femoris musculotendon mechanics during the swing phase of sprinting. *Medicine & Science in Sports & Exercise*, *37*(11), 1931–1938. https://doi.org/10.1249/01.mss.0000176674.42929.de

Thelen, D. G., Chumanov, E. S., Hoerth, D. M., Best, T. M., Swanson, S. C., Li, L., Young, M., & Heiderscheit, B. C. (2005). Hamstring muscle kinematics during treadmill sprinting. *Medicine & Science in Sports & Exercise*, *37*(1), 108–114. https://doi.org/10.1249/01.MSS.0000150078.79120.C8

Timmins, R. G., Shield, A. J., Williams, M. D., Lorenzen, C., & Opar, D. A. (2015). Biceps femoris long head architecture: A reliability and retrospective injury study. *Medicine & Science in Sports & Exercise*, *47*(5), 905–913. https://doi.org/10.1249/MSS.0000000000000507

Ward, S. R., Eng, C. M., Smallwood, L. H., & Lieber, R. L. (2009). Are current measurements of lower extremity muscle architecture accurate? *Clinical Orthopaedics and Related Research*, *467*(4), 1074–1082. https://doi.org/10.1007/s11999-008-0594-8

Yu, B., Queen, R. M., Abbey, A. N., Liu, Y., Moorman, C. T., & Garrett, W. E. (2008). Hamstring muscle kinematics and activation during overground sprinting. *Journal of Biomechanics*, *41*(15), 3121–3126. https://doi.org/10.1016/j.jbiomech.2008.09.005

Zajac, F. E. (1989). Muscle and tendon: Properties, models, scaling, and application to biomechanics and motor control. *Critical Reviews in Biomedical Engineering*, *17*(4), 359–411. http://www.ncbi.nlm.nih.gov/pubmed/2676342

Appendices

Appendix A: Extended modelling methods

A generic musculoskeletal model comprised of 14 segments and 23 degrees of freedom across 12 joints was used to predict hamstring MTU mechanics during the late swing phase of sprinting (Lai et al., 2017). All simulations were performed in OpenSim v3.3. The model has been adapted from the open-source model by Rajagopal et al. (2016) to provide better simulations of movements requiring large hip and knee flexion angles, such as sprinting (Lai et al., 2017). The model was driven by 80 Hill-type MTUs, comprised of a passive and active element in parallel, and an in-series elastic element to represent the tendon (Zajac, 1989). Muscle optimal fibre lengths and pennation angles were based on previously published cadaveric data (Ward et al., 2009) and maximum isometric forces were determined using lower limb muscle volumes from MRI of healthy young adults (Handsfield et al., 2014). The generic properties of the four hamstring muscles (biceps femoris long head, BFlh; biceps femoris short head, BFsh, semimembranosus, SM; semitendinosus, ST) can be found in Table A1.

The generic model was scaled to each individual athlete based on their anthropometry. This included adjustments to segment dimensions, MTU lengths, moment arms and mass and inertia properties of the segments. The maximum isometric force was scaled up by 2.1 times for all muscles in the model, as this was the minimum Scaling factor that allowed all simulations to run successfully and better represented the muscle properties of strong rugby athletes. Maximum contraction velocity was scaled up two times (20 optimal fibre lengths/second). Similar Scaling factors have been used for these parameters in other simulations of running (Thelen, Chumanov, Best, et al., 2005). The subtalar and metatarsophalangeal joints were locked throughout all simulations. Events were placed in the sprint trial data in order to define the late swing phase, beginning at peak knee flexion and ending at foot contact. The late swing phase was identified as the period of interest as this is when hamstring injuries are likely to occur. Marker trajectory and ground reaction force data were both filtered using a low-pass Butterworth filter with a cut off of 15 Hz. Inverse kinematics was then used to calculate a set of generalized coordinates, velocities and accelerations that best match the experimental data by minimizing the sum of squared differences between virtual markers on the model and experimental markers that were placed on the athlete. The resulting kinematic data was filtered at 8 Hz, before net joint torques were calculated using inverse dynamics. A residual reduction algorithm was used to minimize residual forces required at the pelvis due to dynamic inconsistencies between independently collected kinematic and ground reaction force data. Computed muscle control was then used to predict hamstring MTU forces and muscle fibre and tendon lengths. Computed muscle control uses a combination of proportional-derivative control and static optimization to calculate a set of muscle excitations that will drive the model coordinates towards the desired kinematics (Thelen & Anderson, 2006). MTU contraction dynamics were informed by the force-length-velocity properties of muscle and tendon (Zajac, 1989).

Hamstring MTU force was normalized to body mass (N/kg) and PCSA. MTU lengths were expressed as strain (percentage change in length from a standing pose). MTU velocity was calculated as the derivative of length with respect to time. MTU power was the product of MTU force and velocity, expressed relative to body mass (W/kg).

Table A1. Generic properties of the hamstring muscles used in the current study.

	BFlh	BFsh	SM	ST
Maximum isometric force (N) #	2757	1170	4622	1241
Optimal fibre length (m) *	0.098	0.110	0.086	0.193
Pennation angle (deg) *	10.1	15.1	14.6	13.8
Tendon slack length (m)	0.333	0.106	0.335	0.247

BFlh, biceps femoris long head; BFsh, biceps femoris short head; SM, semimembranosus; ST, semitendinosus.

#Maximum isometric force after being scaled up by a factor of 2.1.

*Based on data published by Ward et al. (2009).

Appendix B: Extended simulation results

This Appendix outlines the detailed simulation results, including errors and residual and reserve forces at each step of processing.

Scaling

The root mean square (RMS) marker errors were 1.0 cm and 1.3 cm for Athlete A and Athlete B, respectively.

Inverse kinematics

The RMS error between experimental and model-based coordinate maker positions averaged across three trials was 2.8 cm for Athlete A, and 2.5 cm for Athlete B. RMS errors between 2 and 4 cm are recommended.

Residual Reduction Algorithm

The residual reduction algorithm (RRA) reduced the residual forces and moments applied at the pelvis. These residual loads applied during inverse dynamics pre and post RRA can be found in Tables A1 and A2. RRA reduced residual forces by an average of 95.3% and residual moments by 64.3%. RRA achieves this reduction in residuals through small changes to the kinematic data. The resulting kinematic errors for the leg of interest (right leg) are reported in Table A3. All data is averaged across the three analysed trials for each athlete.

Table A1. Residual forces (N) applied at the pelvis during inverse dynamics pre and post RRA.

	FX Max			FY Max			FZ Max		
	Pre	Post	% Reduction	Pre	Post	% Reduction	Pre	Post	% Reduction
Athlete A	864.2	18.4	97.9	1599.6	159.5	90.0	871.3	45.3	94.8
Athlete B	952.1	12.4	98.7	2013.6	158.9	92.1	1282.3	30.3	97.6
Ave All	908.2	15.4	98.3	1806.6	159.2	91.2	1076.8	37.8	96.5

Table A2. Residual moments (Nm) applied at the pelvis during inverse dynamics pre and post RRA.

	MX Max			MY Max			MZ Max		
	Pre	Post	% Reduction	Pre	Post	% Reduction	Pre	Post	% Reduction
Athlete A	357.7	72.4	79.7	524.6	153.0	70.6	299.6	245.0	18.2
Athlete B	586.2	67.1	88.6	449.6	83.8	81.3	315.8	174.4	44.0
Ave All	472.0	69.8	85.2	487.1	118.4	75.7	307.7	209.7	31.9

Table A3. Kinematic adjustments resulting from RRA in order to reduce the required residual loads.

	Translations (cm)*		Rotations (deg)#	
	Max	RMS	Max	RMS
Athlete A	1.8	1.2	1.3	0.8
Athlete B	2.9	1.7	1.6	1.0
Ave All	2.4	1.4	1.4	0.9

*Translations in the x, y and z direction at the pelvis.
#Rotations at the pelvis and right leg.

Computed Muscle Control

Kinematic tracking errors from computed muscle control (CMC) are reported in Table A4. The magnitude of residual forces and moments applied at the pelvis are shown in Table A5. Reserve actuator contributions to joint moments are displayed in Table A6. All data is averaged across the three analysed trials for each athlete.

Evaluation of predicted muscle activity

Predicted muscle activations were compared to those from previous literature to evaluate the validity of simulations. Typically, these results are analysed with respect to the timing of onset and offset of muscle activity, rather than amplitude of signal. The predicted muscle activities for Athlete A and B are displayed in Figure A1.

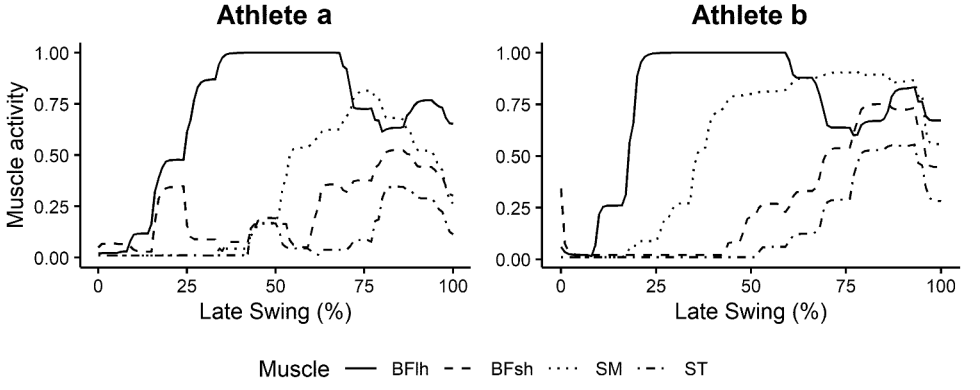

Figure A1. Predicted muscle activations for the hamstrings across the late swing phase.

Several studies have described the muscle activity of the medial and lateral hamstrings during high-speed running. While the hamstrings are active throughout the entire gait cycle, there is very little muscle activity through early and mid-swing, before a large peak in activity during late swing (Chumanov et al., 2011; Higashihara et al., 2015; Yu et al., 2008). The timing of onset in the current study aligns closely with that presented by Schache et al. (2012) and Chumanov et al. (2011) as muscle activity is low at the beginning of the defined late swing phase (mid swing) and increases rapidly throughout late swing. Further, Kyröläinen et al. (1999) reported peak biceps femoris muscle activity between 50 and 100 ms prior to foot strike during maximum velocity sprinting. In the current study, BFlh activation peaked between 50 and 90 ms prior to foot strike for Athlete A, and 70 and 120 ms for Athlete B. Hence, these predicted muscle activations show good agreement with recorded EMG from the literature.

Table A4. Kinematic errors resulting from CMC. These represent the difference between experimental generalized coordinates and those predicted by the model.

	Translations (cm)*		Rotations (deg)#	
	Max	RMS	Max	RMS
Athlete A	0.3	0.2	2.0	1.2
Athlete B	0.2	0.1	1.5	0.8
Ave All	0.3	0.1	1.8	1.0

*Translations in the x, y and z direction at the pelvis.
#Rotations at the pelvis and right leg.

Table A5. Residual forces (N) and moments (Nm) applied at the pelvis during CMC.

	FX		FY		FZ		MX		MY		MZ	
	Max	RMS	Max	RMS	Max	RMS	Max	RMS	Max	RMS	Max	RMS
Athlete A	164.7	69.1	102.3	54.0	140.7	56.4	135.2	58.0	247.7	116.7	105.7	46.9
Athlete B	154.0	48.5	96.0	43.9	174.2	71.5	110.8	50.4	189.1	94.6	74.2	31.6
Ave All	159.3	58.8	99.1	48.9	157.5	64.0	123.0	54.2	218.4	105.7	89.9	39.2

Table A6. Reserve actuator contribution (%) to joint torques in the leg of interest (right leg) during CMC.

	Lumbar			Hip			Knee	Ankle
	Flexion/ Extension	Bending	Rotation	Flexion/ Extension	Adduction/ Abduction	Internal/External Rotation	Flexion/ Extension	Flexion/ Extension
Athlete A	0.3	0.3	0.2	1.2	20.1	84.0	10.1	0.0
Athlete B	0.3	0.2	0.2	0.9	14.7	103.6	4.4	0.0
Ave All	0.3	0.2	0.2	1.0	17.4	93.8	7.2	0.0